Luminescent Materials

Deutsche Ausgabe: DOI: 10.1002/ange.201504786
Internationale Ausgabe: DOI: 10.1002/anie.201504786

Design of Highly Photofunctional Porous Polymer Films with Controlled Thickness and Prominent Microporosity

*Cheng Gu, Ning Huang, Yang Wu, Hong Xu, and Donglin Jiang**

Abstract: *Porous organic polymers allow the integration of various π-units into robust porous π-networks, but they are usually synthesized as unprocessable solids with poor light-emitting performance as a result of aggregation-related excitation dissipation. Herein, we report a general strategy for the synthesis of highly emissive photofunctional porous polymer films on the basis of a complementary scheme for the structural design of aggregation-induced-emissive π-systems. We developed a high-throughput and facile method for the direct synthesis of large-area porous thin films at the liquid–electrode interface. The approach enables the preparation of microporous films within only a few seconds or minutes and allows precise control over their thickness with sub-nanometer precision. By virtue of rapid photoinduced electron transfer, the thin films can detect explosives with enhanced sensitivity to low parts-per-million levels in a selective manner.*

Progress in polymer chemistry over the past decade has had a great effect on the design of porous organic polymers (POPs).[1–3] Despite recent advances, the synthesis of POPs is still based on solution-phase polymerization, which gives rise to insoluble and unprocessable solids as a result of the formation of network structures, thus precluding the fabrication of thin films for applications. Although various π-units have been utilized as monomers for the synthesis of π-electronic POPs, their photofunctionality is quite limited as a result of aggregation-caused excitation-energy dissipation.[1–3] Therefore, POPs are facing two major limitations—lack of processability and poor photofunctionality—which need to be overcome for optoelectronic applications.[1]

Aggregation-induced emission (AIE) is the phenomenon of chromophores becoming emissive in aggregated states. Since the first report by Tang and co-workers in 2001, AIE has emerged as a quickly growing field with broad applications in light-emitting diodes, fluorescence labeling, light harvesting, photonic devices, and chemo- and biosensing.[4] Porous polymers with AIE building blocks have been reported.[5] However, these porous solids are less emissive and lack processability (see Table S1 in the Supporting Information).[5]

In this study, we introduced the concept of AIE to the design of POP networks through the use of a complementary design scheme. In conjunction with the electropolymerization method, we succeeded in the first synthesis of highly luminescent photofunctional POP films. To establish the properties of high emission and photoactivity, we integrated AIE units into the focal core of the π-system (Figure 1a, green part of TPECz), whereas multiple peripheral units (blue parts) were designed for site-specific electropolymerization, and phenylene linkers (purple parts) were employed to introduce twists that help the development of three-dimensional porous skeletons (Figure 1b,c). The electropolymerization of N-substituted carbazoles was established as a polymerization method several decades ago. Nevertheless, this method was not developed until recently for the synthesis of POP films.[6] The development of AIE-based highly emissive photofunctional films simultaneously overcomes the above two limitations faced in the POP field.

The polyTPECz films were produced on electrodes by multicycle cyclic voltammetry (CV) of TPECz (8×10^{-4} M) in a mixture of acetonitrile and CH_2Cl_2 (1:4 v/v) containing the electrolyte tetrabutylammonium hexafluorophosphate with a potential range from −0.8 to 1.03 V at room temperature (see the Supporting Information).[6] Figure 1a shows the CV curves up to 10 cycles. In the first cycle of the positive CV scan, the onset potential of TPECz appeared at 0.97 V, which was attributed to the oxidation of carbazole groups (see Figure S1 in the Supporting Information). As the scan potential increased above 0.97 V, the anodic current increased rapidly and yielded a peak potential at 1.10 V, thus indicating that more carbazole groups were oxidized. During the negative scan, a reductive peak was clearly observed at 0.76 V, which was assigned to the reduction of dimeric carbazole cations (Figure 1d). In contrast, the oxidation and reduction peaks of the tetraphenylethylene (TPE) focal core were observed at potentials of 1.39 and 1.00 V, respectively (see Figure S1). This clear difference in the redox potentials between the focal TPE unit and the carbazole groups is important, because it indicates that polymerization occurred only at the peripheral carbazole groups, whereas the focal TPE unit remained untouched.

In the second cycle, a new oxidative peak appeared at 0.86 V, which was assigned to the oxidation of dimeric carbazoles in the film.[6] The current of this peak increased as the number of cycles increased. This trend was also observed for the reduction peaks. These current-enhancement phenomena reflected the growth of the polyTPECz film

[*] Dr. C. Gu,[+] N. Huang,[+] Y. Wu, Dr. H. Xu, Prof. D. Jiang
Department of Materials Molecular Science, Institute for Molecular Science, National Institutes of Natural Sciences
5-1 Higashiyama, Myodaiji, Okazaki 444-8787 (Japan)
E-mail: jiang@ims.ac.jp
[+] These authors contributed equally.

Supporting information for this article is available on the WWW under http://dx.doi.org/10.1002/anie.201504786.

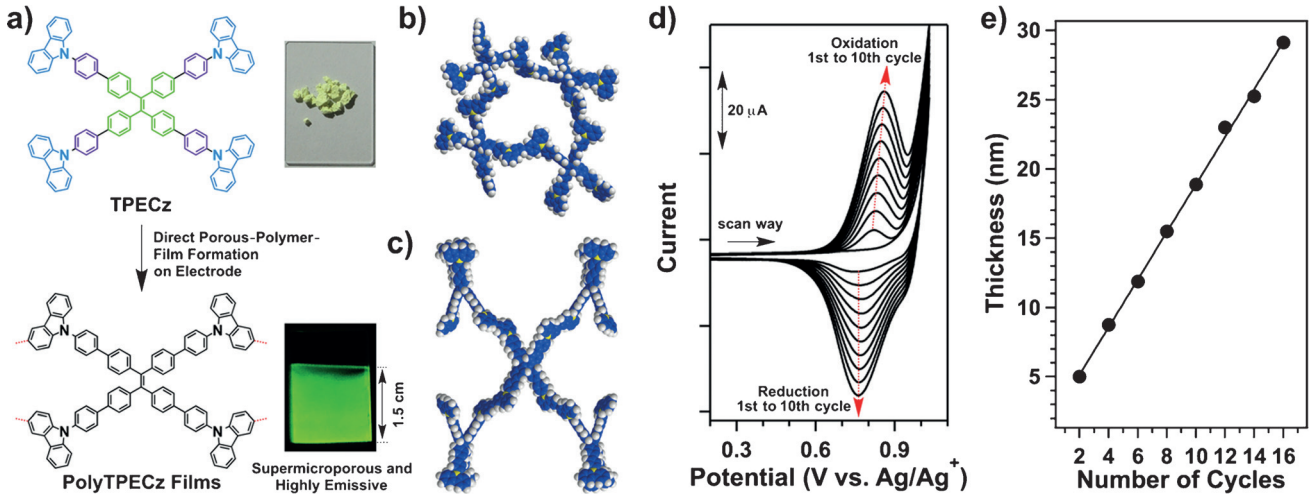

Figure 1. a) Rational design of emissive photofunctional microporous π-networks with an AIE core (green), twisted linkers (purple), and electropolymerizable peripheries (blue), and formation of the films by electropolymerization (dotted red lines indicate connections to the next carbazole unit). The top inset is a photograph of TPECz powder, and the bottom inset is an image of an emissive microporous polyTPECz film. b,c) Optimal closed (b) and open framework (c) of the TPECz-based segments in the π-networks, as simulated by DFT calculations at the B3LYP 6-31G* level (C blue, N yellow, H white). d) CV profiles (1st to 10th cycles) of a solution of TPECz in acetonitrile/CH_2Cl_2 (1:4 v/v) in the presence of the NBu_4PF_6 electrolyte at 25 °C with a scan rate of 0.05 Vs^{-1}. e) Plot of the film thickness versus the CV cycle number.

upon CV cycling (Figure 1 d). After 10 cycles, a transparent green-yellow film had formed on the electrode. Infrared spectroscopy confirmed the formation of dimeric carbazole linkers in the polyTPECz films (see Figure S2).

This method for the direct synthesis of polyTPECz thin films is quite unique. First, it showed high throughput, because the electropolymerization occurred only at the liquid–electrode interface; no bulk polymer solids formed. The preparation of a thin film required only a small amount of the monomer: Experiments carried out on a scale of several milligrams produced hundreds of films with dimensions of 1.5 cm × 2 cm × 10 nm. The method is also rapid and time-saving. The preparation of a film with a thickness of 5 nm was complete within 30 s. Furthermore, the thickness of the films could be controlled by changing the number of CV cycles, whereby each cycle contributed approximately 1.7 nm to the film thickness (Figure 1 e). We prepared films with thicknesses ranging from several nanometers to several micrometers. Finally, the films grew only on the electrode and had the same size and shape as the electrodes; in this study, films with a size of up to 1.5 × 1.5 cm^2 were produced (Figure 1 a, inset).

We conducted Kr sorption isotherm measurements to investigate the porosity of the polyTPECz films and observed that these films were highly porous (Figure 2 a). The Brunauer–Emmett–Teller surface area was evaluated to be as high as 1020 m^2g^{-1}. The pore-size distribution profile (Figure 2 b, black curve) revealed that the pore size was 1.5 nm and that the pore volume was 0.61 cm^3g^{-1} (red curve). High-resolution transmission electron microscopy also confirmed the porous texture of the films (see Figure S3). The films showed a smooth surface morphology, as revealed by field emission scanning electron microscopy (see Figure S4 a). Atomic force microscopy revealed that the thin films (19 nm thick) were flat with a root-mean-square roughness of only 0.32 nm (Figure S4 c).

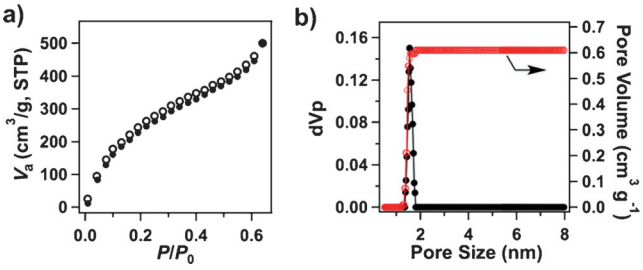

Figure 2. a) Kr sorption isotherm curves for the polyTPECz film at 77 K (filled circles: adsorption, open circles: desorption; STP = standard temperature and pressure). b) Pore-size (black dots) and pore-size-distribution (red circles) profiles of the polyTPECz film.

We next investigated the electronic features of the polyTPECz films. A spin-coated film of TPECz exhibited an absorption band at 331 nm, which was assigned to the π–π* transition of the focal TPE-based unit, and a band at 296 nm, which was assigned to the π–π* transition of the N-substituted carbazole groups (see Figure S5). The polyTPECz films exhibited a red-shifted absorption band at 300 nm that was assigned to the dicarbazole units, whereas the absorption peak of the focal TPE core was retained at 331 nm. Upon excitation at 331 nm, the porous polyTPECz film emitted green luminescence centered at 524 nm (Figure 3 a; see also Figure S6). Similarly, upon excitation at 331 nm, the spin-coated TPECz film emitted at 520 nm.

TPECz as a dilute solution in tetrahydrofuran exhibited an absolute fluorescence quantum yield of only 5 % (Figure 3 b). In contrast, the spin-coated TPECz film had a significantly enhanced absolute quantum yield of 21 % because of the AIE effect.[4] Remarkably, the porous polyTPECz film exhibited an absolute fluorescence quantum yield of 40 %, which was almost twice that of the TPECz

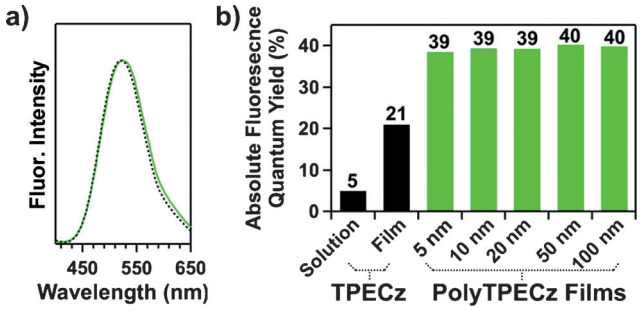

Figure 3. a) Fluorescence spectra of a polyTPECz film (green curve) and spin-coated TPECz film (dotted black curve). b) Absolute fluorescence quantum yields of solutions in tetrahydrofuran of TPECz, a spin-coated TPECz film, and porous polyTPECz films of different thicknesses.

monomer in the spin-coated-film state (Figure 3b). We further investigated the absolute fluorescence quantum yields of the porous films of different thicknesses ranging from 10 to 100 nm. Surprisingly, these films exhibited a constant quantum yield of 40%, irrespective of film thickness. In the polyTPECz films, the TPECz units are linked into networks by covalent bonds, and these linkages further lock the rotation of the TPE units. This structure is the reason for the higher quantum yield of the polyTPECz films as compared to the spin-coated films of the TPECz monomer. The porous films prepared by electropolymerization that have been reported to date are not based on AIE units, and the most emissive had a quantum yield of only 19%.[6c] The integration of AIE units dramatically enhanced the photoluminescence capability, with an increase in the quantum yield to 40%. Notably, the luminescence activity of the porous polyTPECz films is the highest reported for AIE-based porous materials to date; these materials typically have a quantum yield of only a few percent (see Table S1).[5] Owing to their cross-linked nature, the polyTPECz films were robust and retained their luminescence in common organic solvents and various aqueous acidic and basic solutions, thus making them useful as luminescent materials for applications under different conditions.

The porous polyTPECz films are highly photofunctional. Time-resolved fluorescence spectroscopy revealed that a polyTPECz film had a luminescence lifetime of 0.87 ns, whereas the spin-coated monomer film had a luminescence lifetime of 1.01 ns (see Figure S7). We investigated the fluorescence-depolarization profiles, which reflect the occurrence of exciton migration. The TPECz monomer showed a fluorescence-depolarization value of 0.39 (see Figure S8). In contrast, a polyTPECz film (10 nm thick) exhibited significantly depolarized fluorescence with a depolarization value of only 0.07. This observation suggested that the network in the film facilitated exciton migration over the polyTPECz skeleton. Facilitated exciton migration is a key mechanism for enhancing the sensitivity of chemosensing.[7]

The porous polyTPECz films possessed a highly emissive π-skeleton, open, accessible micropores, and a high capacity for rapid exciton migration. These features rendered them able to detect chemicals in a highly sensitive manner. We demonstrated this concept by immersing polyTPECz films in acetonitrile solutions of various nitrobenzene compounds, including 2,4,6-trinitrophenol (TNP), 2,4-dinitrophenol (DNP), 2,4-dinitrotoluene (DNT), 2-nitrophenol (NP), and 2-nitrotoluene (NT), followed by fluorescence spectroscopy of the film. Among these nitro compounds, TNP is designated as an explosive. We utilized polyTPECz films of different thicknesses (10, 20, and 30 nm) for fluorescence sensing. We observed that upon immersion in the solution of TNP in acetonitrile at a low concentration of 50 ppm for only 1 min, the fluorescence of a polyTPECz film with a thickness of 10 nm was quenched by as much as 76% (Figure 4a). The

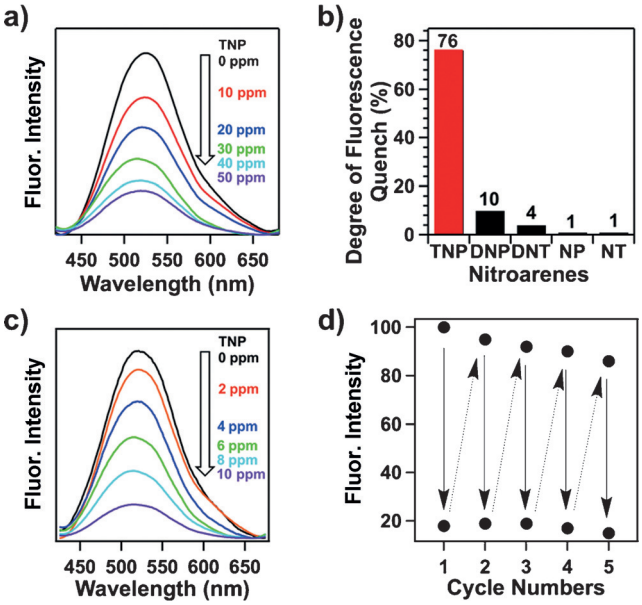

Figure 4. a) Fluorescence spectral change of a 10 nm thick polyTPECz film upon immersion in solutions of TNP in acetonitrile for 1 min. b) Degree of fluorescence quenching of polyTPECz films (10 nm thick) after immersion for 1 min in solutions of various nitroarenes (50 ppm) in acetonitrile. c) Fluorescence spectral change of a 5 nm thick polyTPECz film for sensing TNP. d) Cyclic use of a 10 nm thick polyTPECz film for sensing TNP.

degree of fluorescence quenching decreased as the film thickness was increased to 20 and 30 nm under otherwise identical conditions (see Figure S9). A thicker film emitted stronger luminescence, which required more TNP molecules to quench the fluorescence. To our surprise, the polyTPECz films could discriminate the TNP explosive from other nitrobenzene compounds, such as DNP, DNT, NP, and NT. For example, the degree of fluorescence quenching was only 10, 4, 1, and 1% for DNP, DNT, NP, and NT, respectively (Figure 4b; see also Figure S10). To the best of our knowledge, porous polymers that enable the selective detection of nitroarenes have not been reported previously.[1–3]

Along this line of study, we further investigated the possibility of enhancing the sensitivity by decreasing the film thickness. We synthesized polyTPECz films with a thickness of 5 nm to sense TNP (Figure 4c). These films were extremely sensitive to TNP and exhibited fluorescence quenching by

82 % upon immersion in the TNP solution for only 1 min; the TNP concentration could be further decreased to as low as 10 ppm. Conventional AIE-based polymers function with a sensitivity of several hundreds of parts per million.[5] However, the polyTPECz films with a thickness of 5 nm also retained outstanding selectivity for TMP over DNP, DNT, NP, and NT (see Figures S11 and S12).

The Stern–Volmer quenching constant (k_{SV}) of the film with a thickness of 10 nm was estimated to be $6.4 \times 10^4\,M^{-1}$ for TNP, which was 28 and 81 times the value for DNP ($2.3 \times 10^3\,M^{-1}$) and DNT ($7.9 \times 10^2\,M^{-1}$), respectively (see Figure S13). When the film thickness was decreased to 5 nm, the k_{SV} value increased drastically to $4.04 \times 10^5\,M^{-1}$, thus revealing the excellent sensitivity of the film to TNP (see Figure S14). The chemosensing is related to the level of the lowest unoccupied molecular orbital (LUMO) of the nitroarenes (see Figure S15). The calculated LUMO energy level of TNP was −3.92 eV, which is much lower than that of the polyTPECz skeleton (−2.69 eV), thus providing a strong driving force for the photoinduced electron transfer. In sharp contrast, the LUMO energy levels of NP and NT are −2.19 and −2.31 eV, respectively, which are higher than that of the film and prevented the occurrence of electron transfer.

We used time-resolved fluorescence spectroscopy to elucidate the photochemical dynamics of the films. The polyTPECz film with a thickness of 10 nm in acetonitrile exhibited an average lifetime (τ_0) of 0.78 ns. In the presence of TNP, the lifetime (τ_{DA}) of the polyTPECz film gradually decreased to 0.74, 0.68, 0.59, 0.53, and 0.44 ns as the TNP concentration was increased from 10 to 20, 30, 40, and 50 ppm, respectively (see Figure S16). The pseudo-first-order rate constant of electron transfer from the film to TNP was estimated to be $9.90 \times 10^8\,s^{-1}$ on the basis of the value of ${\tau_{DA}}^{-1} - {\tau_0}^{-1}$. The apparent quenching constant, k_q ($k_q = k_{SV}/\tau_0$), for the polyTPECz film–TNP system was evaluated to be 8.20×10^{13} and $4.75 \times 10^{14}\,M^{-1}s^{-1}$ for films with a thickness of 10 and 5 nm, respectively. This k_q value was three to four orders of magnitude higher than that of collision-based systems ($10^{10}\,M^{-1}s^{-1}$).[8] Such high k_q values have usually been reported for preorganized donor–acceptor systems; in the present system, the TNP molecules can be trapped in the micropores, thus forming an "assembled" electron-donor–acceptor system.

Figure 4d shows the reusability of the polyTPECz film. Approximately the same degree of fluorescence quenching was observed after each cycle, and the fluorescence intensity recovered to a similar level after TNP was removed. By virtue of the cross-linked π-network, the films were robust for cyclic use and retained sensitivity and rapid response.

In summary, we have developed a general strategy for designing highly emissive photofunctional microporous polymer films. The structural design integrates three functional segments, including an AIE core, twisted linkers, and electropolymerizable peripheral units, into well-defined porous π-networks. This high-throughput method for film synthesis enabled elaborate control over the thickness of the films with sub-nanometer precision. The porous films possess a large surface area, are highly green-luminescent, and facilitate exciton migration. The high rate of photoinduced electron transfer renders the films able to detect explosives present at low parts-per-million concentrations in a sensitive and selective manner. The complementary design strategy is widely applicable to many other AIE systems. We envisage that the photofunctional porous films will introduce a new era not only of sensing but also of photocatalysis and photoenergy conversion.

Acknowledgements

This research was supported by a Grant-in-Aid for Scientific Research (A) (24245030) from MEXT of Japan. C.G. is an International Research Fellow of the Japan Society for the Promotion of Science (JSPS).

Keywords: aggregation-induced emission · luminescence · porous polymers · sensors · thin films

How to cite: *Angew. Chem. Int. Ed.* **2015**, *54*, 11540–11544
Angew. Chem. **2015**, *127*, 11702–11706

[1] Y. Xu, S. Jin, H. Xu, A. Nagai, D. Jiang, *Chem. Soc. Rev.* **2013**, *42*, 8012–8031.

[2] a) X. Liu, Y. Xu, D. Jiang, *J. Am. Chem. Soc.* **2012**, *134*, 8738–8741; b) L. Chen, Y. Yang, D. Jiang, *J. Am. Chem. Soc.* **2010**, *132*, 9138–9143; c) N. Huang, Y. Xu, D. Jiang, *Sci. Rep.* **2014**, *4*, 7228: DOI: 10.1038/srep07228; d) L. Chen, Y. Honsho, S. Seki, D. Jiang, *J. Am. Chem. Soc.* **2010**, *132*, 6742–6748; e) F. Xu, X. Chen, Z. Tang, D. Wu, R. Fu, D. Jiang, *Chem. Commun.* **2014**, *50*, 4788–4790; f) Y. Kou, Y. Xu, Z. Guo, D. Jiang, *Angew. Chem. Int. Ed.* **2011**, *50*, 8753–8757; *Angew. Chem.* **2011**, *123*, 8912–8916; g) T. Ben, H. Ren, S. Ma, D. Cao, J. Lan, X. Jing, W. Wang, J. Xu, F. Deng, J. M. Simmons, S. Qiu, G. Zhu, *Angew. Chem. Int. Ed.* **2009**, *48*, 9457–9460; *Angew. Chem.* **2009**, *121*, 9621–9624; h) B. Li, Y. Zhang, D. Ma, Z. Shi, S. Ma, *Nat. Commun.* **2014**, *5*, 5537: DOI: 10.1038/ncomms6537; i) S. Xu, K. Song, T. Li, B. Tan, *J. Mater. Chem. A* **2015**, *3*, 1272–1278; j) A. I. Cooper, *Adv. Mater.* **2009**, *21*, 1291–1295; k) Y. Takashima, V. M. Martínez, S. Furukawa, M. Kondo, S. Shimomura, H. Uehara, M. Nakahama, K. Sugimoto, S. Kitagawa, *Nat. Commun.* **2011**, *2*, 168: DOI: 10.1038/ncomms1170.

[3] a) R. S. Sprick, J.-X. Jiang, B. Bonillo, S. Ren, T. Ratvijitvech, P. Guiglion, M. A. Zwijnenburg, D. J. Adams, A. I. Cooper, *J. Am. Chem. Soc.* **2015**, *137*, 3265–3270; b) Y. Xie, T.-T. Wang, X.-H. Liu, K. Zou, W.-Q. Deng, *Nat. Commun.* **2013**, *4*, 1960: DOI: 10.1038/ncomms2960; c) Q. Chen, M. Luo, P. Hammershøj, D. Zhou, Y. Han, B. W. Laursen, C.-G. Yan, B.-H. Han, *J. Am. Chem. Soc.* **2012**, *134*, 6084–6087; d) P. Katekomol, J. Roeser, M. Bojdys, J. Weber, A. Thomas, *Chem. Mater.* **2013**, *25*, 1542–1548; e) L. Pan, Q. Chen, J.-H. Zhu, J.-G. Yu, Y.-J. He, B.-H. Han, *Polym. Chem.* **2015**, *6*, 2478–2487; f) X. Zhu, S. M. Mahurin, S.-H. An, C.-L. Do-Thanh, C. Tian, Y. Li, L. W. Gill, E. W. Hagaman, Z. Bian, J.-H. Zhou, J. Hu, H. Liu, S. Dai, *Chem. Commun.* **2014**, *50*, 7933–7936; g) S. Qiao, Z. Du, R. Yang, *J. Mater. Chem. A* **2014**, *2*, 1877–1885; h) J. Luo, X. Zhang, J. Zhang, *ACS Catal.* **2015**, *5*, 2250–2254; i) M. Saleh, S. B. Baek, H. M. Lee, K. S. Kim, *J. Phys. Chem. C* **2015**, *119*, 5395–5402.

[4] a) J. Luo, Z. Xie, J. Lam, L. Cheng, H. Chen, C. Qiu, H. S. Kwok, X. Zhan, Y. Liu, D. Zhu, B. Z. Tang, *Chem. Commun.* **2001**, 1740–1741; b) M. Wang, G. Zhang, D. Zhang, D. Zhu, B. Z. Tang, *J. Mater. Chem.* **2010**, *20*, 1858–1867; c) Y. Hong, J. W. Y. Lam, B. Z. Tang, *Chem. Soc. Rev.* **2011**, *40*, 5361–5388; d) Y. Dong, J. W. Y. Lam, A. Qin, J. Liu, Z. Li, B. Z. Tang, J. Sun, H. S. Kwok,

Appl. Phys. Lett. **2007**, *91*, 011111; e) H. Tong, Y. Hong, Y. Dong, M. Häußler, J. W. Y. Lam, Z. Li, Z. Guo, Z. Guo, B. Z. Tang, *Chem. Commun.* **2006**, 3705 – 3707; f) Z. Zhao, J. W. Y. Lam, B. Z. Tang, *J. Mater. Chem.* **2012**, *22*, 23726 – 23740.

[5] a) Y. Xu, L. Chen, Z. Guo, A. Nagai, D. Jiang, *J. Am. Chem. Soc.* **2011**, *133*, 17622 – 17625; b) Y. Xu, A. Nagai, D. Jiang, *Chem. Commun.* **2013**, *49*, 1591 – 1593; c) Q. Chen, J.-X. Wang, F. Yang, D. Zhou, N. Bian, X.-J. Zhang, C.-G. Yan, B.-H. Han, *J. Mater. Chem.* **2011**, *21*, 13554 – 13560; d) A. Bhunia, V. Vasylyeva, C. Janiak, *Chem. Commun.* **2013**, *49*, 3961 – 3963; e) J. Lu, J. Zhang, *J. Mater. Chem. A* **2014**, *2*, 13831 – 13834; f) N. B. Shustova, B. D. McCarthy, M. Dincå, *J. Am. Chem. Soc.* **2011**, *133*, 20126 – 20129; g) N. B. Shustova, T.-C. Ong, A. F. Cozzolino, V. K. Michaelis, R. G. Griffin, M. Dincå, *J. Am. Chem. Soc.* **2012**, *134*, 15061 – 15070; h) Q. Gong, Z. Hu, B. J. Deibert, T. J. Emge, S. J. Teat, D. Banerjee, B. Mussman, N. D. Rudd, J. Li, *J. Am. Chem. Soc.* **2014**, *136*, 16724 – 16727; i) Z. Wei, Z.-Y. Gu, R. K. Arvapally, Y.-P. Chen, Jr., R. N. McDougald, J. F. Ivy, A. A. Yakovenko, D. Feng, M. A. Omary, H.-C. Zhou, *J. Am. Chem. Soc.* **2014**, *136*, 8269 – 8276; j) W. Xie, S.-R. Zhang, D.-Y. Du, J.-S. Qin, S.-J. Bao, J. Li, Z.-M. Su, W.-W. He, Q. Fu, Y.-Q. Lan, *Inorg. Chem.* **2015**, *54*, 3290 – 3296.

[6] a) C. Gu, Y. Chen, Z. Zhang, S. Xue, S. Sun, K. Zhang, C. Zhong, H. Zhang, Y. Pan, Y. Lv, Y. Yang, F. Li, S. Zhang, F. Huang, Y. Ma, *Adv. Mater.* **2013**, *25*, 3443 – 3448; b) C. Gu, N. Huang, J. Gao, F. Xu, Y. Xu, D. Jiang, *Angew. Chem. Int. Ed.* **2014**, *53*, 4850 – 4855; *Angew. Chem.* **2014**, *126*, 4950 – 4955; c) C. Gu, N. Huang, F. Xu, J. Gao, D. Jiang, *Sci. Rep.* **2015**, *5*, 8867: DOI: 10.1038/srep08867; d) C. Gu, T. Fei, Y. Lv, T. Feng, S. Xue, D. Lu, Y. Ma, *Adv. Mater.* **2010**, *22*, 2702 – 2705; e) C. Gu, T. Fei, L. Yao, Y. Lv, D. Lu, Y. Ma, *Adv. Mater.* **2011**, *23*, 527 – 530; f) D. Becker, N. Heidary, M. Horch, U. Gernert, I. Zebger, J. Schmidt, A. Fischer, A. Thomas, *Chem. Commun.* **2015**, *51*, 4283 – 4286; g) A. Palma-Cando, U. Scherf, *ACS Appl. Mater. Interfaces* **2015**, *7*, 11127 – 11133; h) P. Lindemann, M. Tsotsalas, S. Shishatskiy, V. Abetz, P. Krolla-Sidenstein, C. Azucena, L. Monnereau, A. Beyer, A. Gölzhäuser, V. Mugnaini, H. Gliemann, S. Bräse, C. Wöll, *Chem. Mater.* **2014**, *26*, 7189 – 7193.

[7] a) D. T. McQuade, A. E. Pullen, T. M. Swager, *Chem. Rev.* **2000**, *100*, 2537 – 2574; b) J.-S. Yang, T. M. Swager, *J. Am. Chem. Soc.* **1998**, *120*, 5321 – 5322.

[8] D. A. Olley, E. J. Wren, G. Vamvounis, M. J. Fernee, X. Wang, P. L. Burn, P. Meredith, P. E. Shaw, *Chem. Mater.* **2011**, *23*, 789 – 794.

Received: May 27, 2015
Published online: July 31, 2015

